



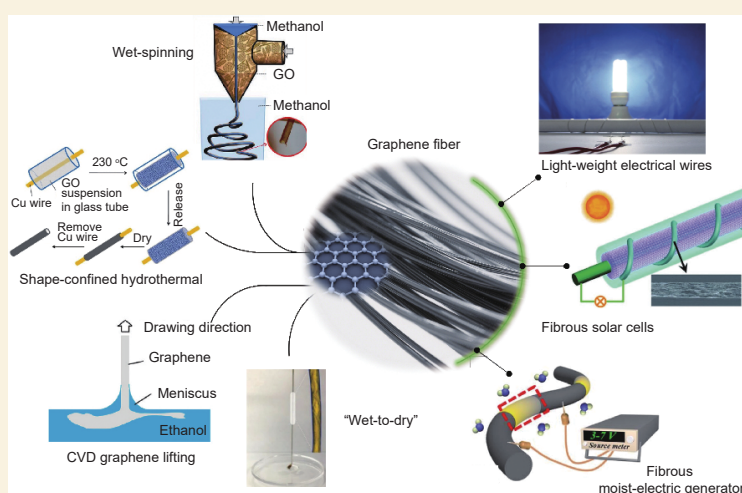
# Wearable energy harvesters based on graphene fibers

Guang Tianlei, Cheng Huhu\*, Qu Liangti

(State Key Laboratory of Flexible Electronics Technology, Key Laboratory of Organic Optoelectronics & Molecular Engineering, Ministry of Education, Department of Chemistry, Tsinghua University, Beijing 100084, China)

**Abstract:** Graphene fibers (GFs) have demonstrated high strength, high electrical and thermal conductivity, mechanical flexibility, chemical stability, and good functionality, etc. at the macro-scale, and have been used in many different fields, particularly next-generation wearable and flexible devices. This review provides an overview of recent advances in the fabrication of GFs, including wet spinning, confined hydrothermal synthesis, chemical vapor deposition, and other emerging techniques. Special emphasis is placed on the development of GF-based devices that convert solar, thermal, or moisture energy from the environment into electrical energy. The working principles, structural design, and performance of these devices are summarized and current challenges and prospects for their use in wearable energy systems are detailed.

**Key words:** Two-dimensional materials; Graphene fiber; Energy harvesters; Fibrous device; Moist-electric generator



## 1 Introduction

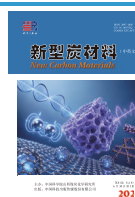
Graphene, a two-dimensional (2D) honeycomb carbon material, has high electron mobility ( $2 \times 10^5 \text{ cm}^2/(\text{V}\cdot\text{s})$ )<sup>[1]</sup>, excellent thermal conductivity ( $5 \times 10^3 \text{ W}/(\text{m}\cdot\text{K})$ )<sup>[2]</sup>, large surface area ( $2.63 \times 10^3 \text{ m}^2/\text{g}$ )<sup>[3]</sup>, and promising mechanical elasticity (1 TPa) and stiffness ( $340 \text{ N}/\text{m}$ )<sup>[4]</sup>. Assembling atomic-thin graphene sheets into functional macroscopic fibers has attracted much attention because of the numerous potential applications in light-weight aircraft, wearable or foldable electronics, advanced energy devices and so on. Because of the irregular size/shape of 2D graphene sheets and the complexities involved in their layer-by-layer assembly<sup>[4]</sup>, great efforts have been dedicated to achieving the construction of GF. For example, in 2011, a wet spinning method was developed to fabricate graphene oxide (GO) fiber based on the formed orientated GO liquid crystal (LC) during flow process for the first time<sup>[5]</sup>. Then, graphene fibers (GFs) of

several meters in length were obtained after chemical reduction or high-temperature treatment. Dong et al. prepared electrically conductive GF directly from GO solution through the space-confined hydrothermal strategy<sup>[6]</sup>. To date, the mechanical strength of GF has reached approximately 3.4 GPa, nearly 10 times greater than that of the GF produced in 2011<sup>[7]</sup>. Meanwhile, the electrical conductivity of GF have also reached about  $8 \times 10^5 \text{ S}/\text{m}$  and a thermal conductivity of  $1290 \text{ W}/(\text{m}\cdot\text{K})$ <sup>[8]</sup>, respectively. Importantly, the ability to tune chemical composition and physical structure has endowed GF with diversified functional properties, including high flexibility, stretchability, charge storage capacity, energy conversion capacity and so on<sup>[9–10]</sup>,

Received: May 02, 2025

Revised: January 29, 2026

Accepted: January 30, 2026



which will subsequently provide unconventional solutions for next-generation technologies by leveraging graphene-based fiber<sup>[11–14]</sup>.

As illustrated in Fig. 1, the development of GF follows a systematic research framework encompassing synthesis, optimization, structure-property relationships, and applications. The synthesis of GFs primarily relies on wet spinning of GO, hydrothermal methods and chemical vapor deposition (CVD), where key factors such as diamine ion bridging and interlayer interactions play crucial roles in determining the material's fundamental characteristics. Subsequent optimization through wet-spinning techniques allows precise control over microstructural features and morphological attributes, while concentration adjustments and defect engineering at micro- and nano-scales further enhance material performance. Understanding the intricate structure-property relationships is essential for tailoring GFs' mechanical strength, electrical conductivity and porosity. These engineered properties ultimately enable advanced applications ranging from light-weight electrical wires to fibrous energy harvesters, including fibrous solar cells, thermoelectric generator (TE), moist-electric generator (MEG). This

review aims to provide a comprehensive discussion on the fabrication of GFs and related fibrous energy harvesters (Fig. 1).

## 2 Fabrication of GF

### 2.1 Wet-spinning

It is difficult to directly disperse graphene sheets in water or organic solvents, therefore, GO with oxygen-rich functional groups was initially employed for GF fabrication. When increasing the concentration of GO dispersion to about 3 mg/mL, a typical LC started to be shown (Fig. 2a)<sup>[5]</sup>. Based on this, a wet-spinning method was developed for producing GO fibers by Gao's group<sup>[9]</sup>. The progress from the initial GO LC to the fully formed fiber is a multifaceted process that can be delineated into 3 distinct stages. Initially, the process begins with the flow-induced unidirectional alignment of the GO sheets (stage I in Fig. 2b). At this stage, GO sheets, which are originally distributed randomly within the three-dimensional (3D) space of the stable GO LC, are realigned along the flow direction. This alignment is crucial for homogenizing the orientational order of the GO sheets, which is a prerequisite for achieving a uniform fiber structure. After the

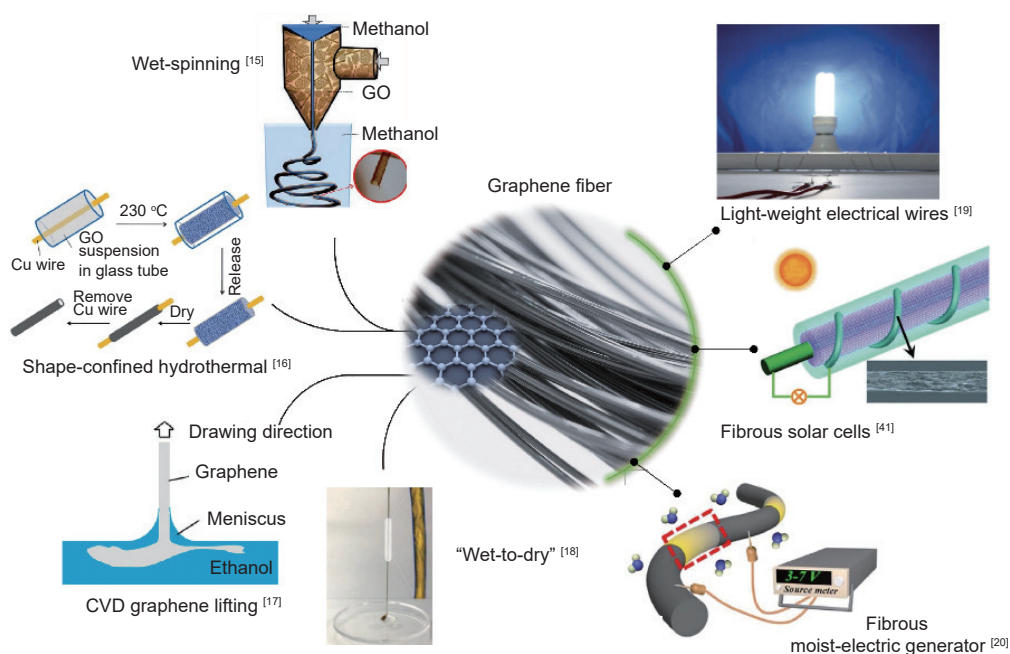


Fig. 1 Fabrication of GFs for fibrous energy harvesters. (Reprinted with permission, Copyright 2013, American Chemical Society<sup>[15]</sup>; Copyright 2012, American Chemical Society<sup>[16]</sup>; Copyright 2011, American Chemical Society<sup>[17]</sup>; Copyright 2018, Wiley<sup>[18]</sup>; Copyright 2016, Wiley<sup>[19]</sup>; Copyright 2013, Wiley<sup>[41]</sup>; Copyright 2017, Elsevier<sup>[20]</sup>)

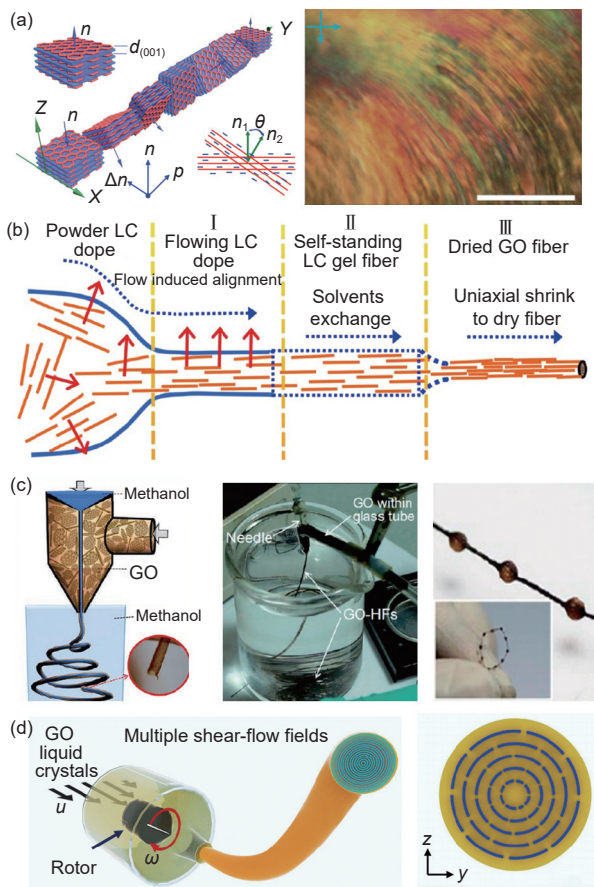


Fig. 2 The wet spinning technique and diverse approaches for augmenting the mechanical characteristics of GFs. (a) Proposed model for one pitch of GO LC (left). The vectors ( $n_s$ ) of the lamellar blocks rotate anticlockwise along the helical axis. Polarized optical microscopy images between crossed polarizers of GO LCs in lateral domains (right). Reprinted with permission, Copyright 2011, Nature Publishing Group<sup>[5]</sup>. (b) Evolution of the microstructural composition of graphene oxide fibers throughout the wet spinning process. Reproduced with permission, Copyright 2014, American Chemical Society<sup>[9]</sup>. (c) A schematic depiction of the apparatus employing a dual-capillary spinneret for the direct fabrication of GFs. Reproduced with permission, Copyright 2014, American Chemical Society<sup>[13]</sup>. (d) Diagram displays the ideally concentric configuration achieved by bidirectionally enhancing the organization of assembly. Reproduced with permission, Copyright 2024, Nature Publishing Group<sup>[14]</sup>

alignment of GO sheets, the process transitions into the second stage (stage II), which entails a crucial solvent exchange between the coagulation baths and GO LC, leading to the formation of self-supporting GO gel fibers. Then, a wet-drawing procedure was employed to further enhance the regular alignment of the GO sheets along the fiber axis, thereby contributing to the mechanical strength and structural integrity of GO gel fibers. The third stage (stage III) is characterized by the drying process, during which the evap-

oration of solvents induces the radial buckling of the GO sheets and shrinkage of GO gel fibers to the compact stacking of the solid GO fibers. The obtained GO fiber from GO LC often exhibited a wrinkled surface morphology. Finally, GF with the desired mechanical and morphological characteristics was obtained after high-temperature treatment or chemical reduction.

Fu et al. further demonstrated that the efficacy of GFs is contingent upon numerous factors, including size and orientation of GO sheets, inter-sheet interactions, and imperfections in GFs<sup>[10]</sup>. By using GO sheets with large size, GFs with significantly improved mechanical properties, including enhanced tensile modulus and flexibility, have been prepared. A notable improvement in the orientation of the graphene sheets within the fibers was when employing GO sheets with  $\sim 23 \mu\text{m}$  size<sup>[8]</sup>. A significant challenge arises from the folding of these GO sheets, which introduces a multitude of pores within the fiber structure that weaken the mechanical properties of GF by creating points of structural inconsistency. Small GO sheets ( $\sim 0.8 \mu\text{m}$ ) result in a substantially dense internal structure. However, this leads to a chaotic and poorly oriented internal structure. To address these challenges, the innovative approach involved the combination of both large and small GO sheets in the spinning solution<sup>[12]</sup>. Large GO sheets guided and enhanced the orientation of the structure, while the small sheets filled the gaps, preventing the formation of weakening pores. This synergistic approach resulted in a highly oriented GF, achieving a strength of 1.08 GPa. Xu et al. introduced a comprehensive and synergistic defect engineering strategy aimed at mitigating potential imperfections across all scales, thereby maximizing the inherent capabilities of GFs in a production-viable manner<sup>[13]</sup>. This approach encompasses 3 distinct strategies with a focused emphasis on defect management throughout: (1) the wet spinning of GO LCs with continuous stretching to ensure a uniform orientation of graphene along the fiber axis; (2) refining the radial dimensions by adjusting the concentration of the spinning solution and the nozzle diameter to produce ultrafine GO fibers with minimal core-

sheath structure defects, orientation boundaries and voids; (3) employing high-temperature graphitization to refine the atomic structure of graphene. GFs developed through this method exhibited exceptionally high stiffness of  $\sim 282$  GPa, a mechanical tensile strength of  $\sim 1.45$  GPa, significant electrical conductivity ( $\sim 0.8 \times 10^6$  S/m), and outstanding ampacity ( $\sim 2.3 \times 10^{10}$  A/m<sup>2</sup>)<sup>[13]</sup>.

Advancing the interfacial interactions of GO sheets is a pivotal aspect in enhancing the overall mechanical properties of fibers<sup>[21–25]</sup>. The integration of phenolic carbon contributes to the densification of GFs by mitigating defects and amplifying the interfacial interaction between inner graphene sheets via the formation of new carbon-carbon bonds. Meanwhile, the integration of metal ions, especially calcium ions (Ca<sup>2+</sup>), into the GO dispersion will create strong bonds at the interface of the graphene layers by ion cross-linking. Furthermore, organic materials such as polydopamine, chitosan and phenolic resin, also act as crosslinking agents to form networks that interlock with the graphene sheets in GFs<sup>[26]</sup>.

This crosslinking process is crucial as it not only enhances the binding force between the layers but also imparts additional properties to the fibers. For instance, polydopamine might contribute to improved environmental stability, while phenolic resin could enhance thermal resistance. Ding et al. introduced a scalable method to fabricate high-performance graphene fibers by covalently bridging GO edges with aromatic amide bonds via wet-spinning route. The resulting fibers achieve remarkable mechanical strength (3.54 GPa) and conductivity ( $1.5 \times 10^5$  S/m) at room temperature, outperforming conventional graphene fibers. The edge-bridging strategy enhances  $\pi$ - $\pi$  stacking and electron conjugation while enabling industrial-scale production, offering promising applications in lightweight composites and advanced electronics<sup>[27]</sup>. The potential of these materials promotes the applications of GFs in different fields like biomedicine, electronics, energy storage and so on.

The innovation in wet-spinning process greatly enriched the physical morphologies of GFs. For ex-

ample, dual-capillary coaxial spinning produced a hollow GF or necklace-like GF with designed structures by inserting air into the inner capillary and GO dispersion in the ring-like space between two capillaries (Fig. 2c)<sup>[15]</sup>. Aligned distribution of GO sheets in GF can also be achieved by optimizing shear forces along the fiber axis by employing flat filament nozzles. Li et al. introduced a novel bidirectional assembly order enhancement, significantly elevating the mechanical and thermal properties of GFs (Fig. 2d). Utilizing multiple shear-flow fields, they achieved a concentric arrangement of GO sheets and axial alignment, leading to optimized sheets organization, densification, and crystallization within GFs with an ultrahigh modulus of  $\sim 901$  GPa and thermal conductivity of 1660 W/(m·K), suggesting broader scientific and technological implications<sup>[14]</sup>. These efforts collectively underscore the critical role of sheet orientation, interfacial engineering, and defect control in unlocking the full mechanical and functional potential of graphene fibers fabricated via wet spinning.

## 2.2 Shape-confined hydrothermal method

In 2012, Dong et al. fabricated GFs directly from GO dispersion by a shape-confined hydrothermal method for the first time<sup>[6]</sup>, by sealing  $\sim 8$  mg/mL GO dispersion in a one-dimensional (1D) glass pipeline ( $\sim 0.4$  mm in inner diameter) and thermally treating at 230 °C for 2 h. The dimensions of GFs, including diameter and length, can be controlled by varying the pipeline's dimensions or adjusting the GO suspension's concentration (Fig. 3a-c). Remarkably,  $\sim 1$  mL of GO dispersion can yield a GF up to  $\sim 6$  m long. This shape-confined hydrothermal process results in tightly stacked graphene layers, giving the GFs considerable tensile strength of  $\sim 180$  MPa. The stabilization of GO dispersions leads to a turbulent state when exposed to elevated temperatures. This turbulence facilitates the detachment of oxygen-containing functional groups from GO sheets, resulting in a notable decrease in the absolute zeta potential of the GO dispersion. The subsequent reduction in electrostatic repulsion among the GO sheets encourages their aggregation along with the 1D glass pipeline and leads to the

formation of a gel-like fiber structure. Then, a compact GF was fabricated upon further drying. The properties of the resulting GFs can be easily regulated by controlling the hydrothermal conditions, such as the temperature and the composition of GO dispersion. Furthermore, the versatility of this method allows for the exploration of GO dispersions with other functional materials for the design and fabrication of GFs with customized components and architectures. For example, by introducing a removable wire-type template inside the 1D glass pipeline in the shape-confined hydrothermal method, hollow functional GFs with 1, 2, 3, or 4 channels can be fabricated (Fig. 3d and e)<sup>[16]</sup>. A scalable shape-confined hydrothermal method for synthesizing GFs modified by single-walled carbon nanotube (SWNT) was developed by injecting SWNT/GO mixed dispersion in a fused-silica capillary column microreactor from one end by

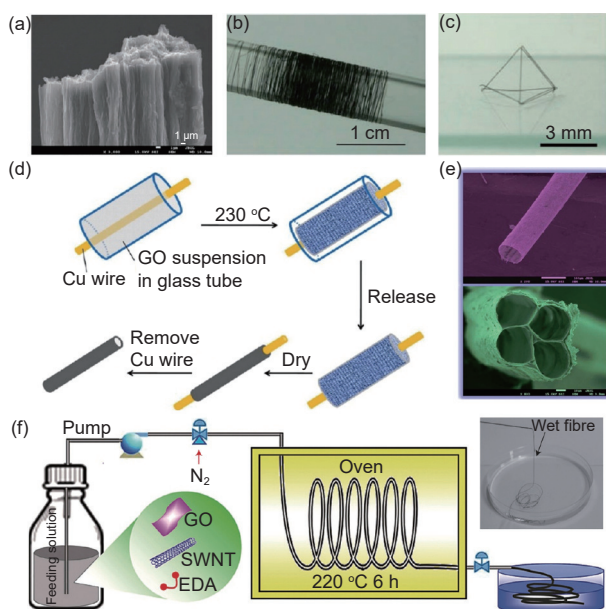


Fig. 3 Shape-confined hydrothermal method. (a) Scanning electron microscopy (SEM) images of the intentionally fractured segment of a GF. (b) An image showcasing dry GFs wound in a bundle around a glass rod. (c) The 3D geometric configurations of GFs. Reproduced with permission, Copyright 2012, Wiley<sup>[6]</sup>. (d) Scheme of the fabrication process of graphene microtubings. (e) SEM images illustrating multichannel graphene microtubings, featuring channel counts ranging from 1 to 4 (utilizing a Cu wire with a diameter of 40 μm), respectively. Reproduced with permission, Copyright 2012, American Chemical Society<sup>[16]</sup>. (f) The fiber was synthesized by injecting a homogeneous solution comprised of acid-oxidized SWNTs, graphene oxide (GO), and ethylenediamine (EDA) by a pump into a flexible silica capillary column. Reproduced with permission, Copyright 2014, Nature Publishing Group<sup>[28]</sup>

Chen et al<sup>[28]</sup>. After heating the dispersion to 220 °C, the reduction of GO to graphene occurs, simultaneously facilitating the bonding between SWNT and graphene sheets. Then, GFs can continuously output from the other end of fused-silica capillary. These novel hydrothermal techniques not only enable precise control over the dimensions and structural properties of GFs directly but also open up new possibilities for creating intricate and multifunctional GFs (Fig. 3f). Such tunability and scalability highlight the hydrothermal method as a promising strategy for mass production and customization of GFs for various application scenarios.

### 2.3 CVD method

The ability of CVD method to produce single-layered and few-layered graphene on catalyst substrates has been a cornerstone in the advancement of graphene technology<sup>[17]</sup>. This has also been utilized to prepare GF with perfectly-honeycomb carbon atomic arrangement. Typically, polycrystalline nickel (Ni) films undergo initial annealing in an argon/hydrogen (Ar/H<sub>2</sub>) environment at temperatures ranging from 900 to 1000 °C to enlarge grain size, followed by exposure to a hydrogen/methane (H<sub>2</sub>/CH<sub>4</sub>) gas mixture<sup>[29]</sup>. During this phase, hydrocarbons decompose, allowing carbon atoms to diffuse into the Ni film and form a solid solution owing to the relatively high carbon solubility of Ni at high temperatures. As the temperature drops during the cooling phase, carbon atoms migrate out of the Ni–C solid solution and precipitate on the Ni surface, leading to the formation of graphene (Fig. 4a). The CVD method applied to synthesize GFs, can avoid the complex reduction process of GO typically required in wet spinning methods. This thermodynamic preference necessitates alternative approaches to achieve the desired 1D fiber structure. To address this challenge, researchers employ fibrous templates as a scaffold for GF growth. These templates guide the carbon species into a macroscopic 1D structure, effectively overcoming the natural inclination to form planar arrangements. Dai et al. used copper wire as a substrate for CVD growth of hollow multilayer graphene tubes. These tubes were then transformed into macroscopic porous GFs by re-

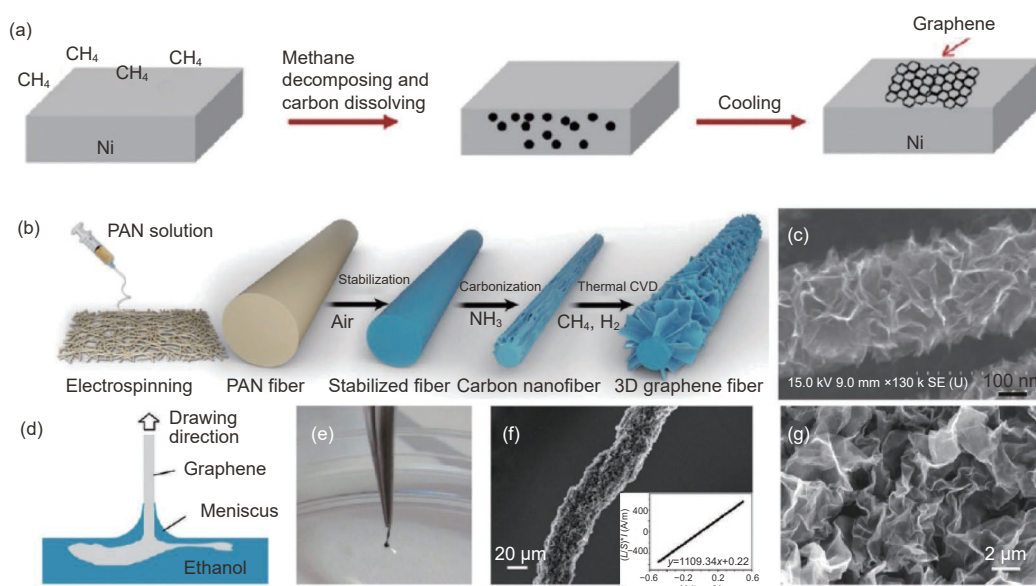


Fig. 4 Chemical vapor deposition method. (a) Schematic representation of the synthesis of graphene on a nickel substrate. Reproduced with permission, Copyright 2013, American Chemical Society<sup>[29]</sup>. (b, c) A schematic depiction of the fabrication procedure for 3D GFs. Reproduced with permission, Copyright 2018, Wiley<sup>[31]</sup>. (d-g) A schematic representation of the self-assembly process from CVD graphene to fiber. Reproduced with permission, Copyright 2011, American Chemical Society<sup>[17]</sup>

moving the copper in an iron chloride (FeCl<sub>3</sub>) and hydrochloric acid (HCl) solution, and continuously drawing the graphene tube out of the liquid<sup>[30]</sup>.

Another strategy is growing graphene nanosheets on pre-carbonized fibers, specifically using polyacrylonitrile (PAN) as a precursor (Fig. 4b and c)<sup>[31]</sup>. This approach yields three-dimensional (3D) GFs characterized by discrete graphene sheets on their surface. The process involves carbonizing PAN fibers and treating them with ammonia, followed by the growth of 3D graphene sheets by the CVD method. This method shows significant advantages over liquid-phase self-assembly or other template methods. Meanwhile, at the graphene growth temperatures (<1200 °C), complete graphitization of the polymer precursor fibers could not be achieved, leading to the presence of defect sites. These defects result in a gap in electrical and thermal conductivity when compared to ideal GFs. Future optimization of the growth conditions and alternative materials or methods could close the gap in the properties of the resulting GFs. Li et al. 's innovation in creating porous GFs using the thin graphene film lift method highlights the importance of precise methodology in material science (Fig. 4d-g). This process underscores the intricate balance of

forces at play, specifically the surface tensions at the solid-liquid, gas-solid and gas-liquid interfaces<sup>[17]</sup>. By manipulating these forces, researchers can control the fiber's characteristics, including its conductivity, which reaches approximately 1000 S/m. This level of conductivity opens up new possibilities for GFs in various electrical applications. Li et al. presented a novel approach for fabricating graphene-coated alumina fibers and fabrics (GAF/GAFF) through CVD on commercial alumina substrates. The resulting GAFF material combines multiple advantageous properties, including adjustable electrical resistance (1–15000 Ω/sq), exceptional mechanical strength (>1.5 GPa), lightweight construction, flexibility, and a multi-scale structural design. These characteristics make it particularly valuable for thermal management applications and electromagnetic shielding solutions<sup>[32]</sup>. Overall, the CVD-based approach enables precise structural control at the atomic level, offering a route to fabricate highly ordered GFs with superior electronic performance, albeit with higher complexity and cost.

#### 2.4 Other strategies

The direct extrusion of high concentrations of GO LCs into air is a streamlined and potentially cost-

effective dry-spinning approach to fabricate GFs (Fig. 5a). High concentrations ensure the formation of viscoelastic GO LC gels, which are critical for the fiber's structural integrity. The increased LC domain size at higher concentrations aids the achievement of better alignment of GO under shear stress, which is an essential factor for the fiber's strength and consistency<sup>[34]</sup>. Meanwhile, the solvent choice in dry-spinning plays a crucial role in the fiber's quality. Solvents with low surface tension and high saturated vapor pressure, like CH<sub>3</sub>OH, C<sub>2</sub>H<sub>5</sub>OH, (CH<sub>3</sub>)<sub>2</sub>CO and C<sub>4</sub>H<sub>8</sub>O(THF), are preferred<sup>[33]</sup>. These solvents facilitate quicker solidification of GO gel fibers, crucial for maintaining the integrity and uniformity of the fibers. Research into new solvent formulations or mixtures could further enhance the quality and properties of the spun GFs. Although dry-spun GFs have some limitations in mechanical strength due to microvoids and core-shell structures, they exhibit high toughness (up to 19.12 MJ/m<sup>3</sup>) and flexibility. Drawing inspiration from the biological natural silk production process<sup>[35–36]</sup>, a novel 'wet-to-dry' hybrid spinning technique (where GO liquid crystals are first aligned in a wet phase and then rapidly solidified by solvent evaporation, mimicking natural silk production) has been devised, ensuring the conversion of nearly all GO into fiber form. At the juncture where 2 droplets—one containing GO and the other polyethyleneimine—meet, the interaction of these oppositely charged entities in their aqueous states leads to binding (Fig. 5b). Following this, one of the components engages and draws the point of interfacial convergence of the droplets, creating a slender vertical liquid column. Within this column, GO complexes are subjected to shear forces, prompting their alignment into a finely spun fiber. When compared to conventional wet-spinning techniques, this innovative wet-to-dry approach is markedly more energy-efficient, characterized by its straightforward methodology, absence of chemical waste, and the near-total conversion of GO precursors into fibers.

The use of a graphitic tip as a positive electrode in a GO colloidal solution is a unique application of

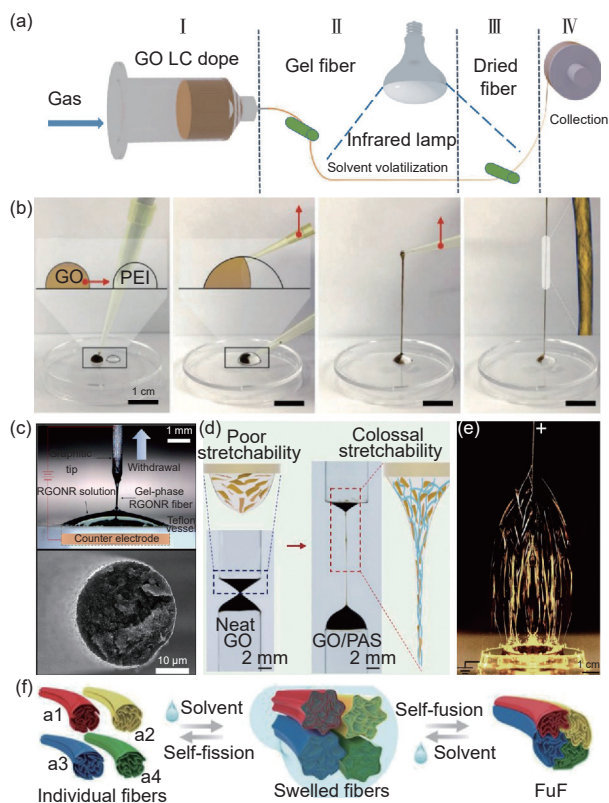


Fig. 5 (a) A schematic illustration of the dry spinning process utilizing a concentrated organic dispersion of GO. Reproduced with permission, Copyright 2017, Royal Society of Chemistry<sup>[34]</sup>. (b) A schematic illustration of procedures for the synthesis of GFs. Reproduced with permission, Copyright 2018, Wiley<sup>[18]</sup>. (c) Image depicting the formation of a gel-phase reduced graphene oxide nanoribbon fiber from a solution throughout the drawing phase. Reproduced with permission, Copyright 2012, IOP publications<sup>[37]</sup>. (d) The juxtaposition of elongation statuses and compositional diagrams for pure GO and GO/PAS spinning solutions. (e) Image depicting the elongation of continuous jet threads emanating from a spinneret nozzle. Reproduced with permission, Copyright 2022, Springer publications<sup>[38]</sup>. (f) A schematic representation of the solvent-induced, precisely reversible self-fusion and self-fission processes of GO fibers. Reprinted with permission, Copyright 2021, The American Association for the Advancement of Science<sup>[39]</sup>

electrophoretic principles in GF production (Fig. 5c)<sup>[37]</sup>. Research into the interplay of electrostatic, van der Waals forces, and  $\pi$ - $\pi$  stacking could provide insights into controlling GF dimensions and properties more precisely. Gao et al. also presented a technique in the field of fabrication of GF by electrospinning from the mixture of GO and polyacrylate sodium (PAS)<sup>[38]</sup>, resulting in GFs with exceptional electronic quality and crystallinity (Fig. 5d and e). Recently, Chang et al. demonstrated a method for the reversible assembly of GO microfibers via solvent-triggered fusion and fission<sup>[39]</sup>. This process allows for

the seamless merging and separation of macroscopic fibers, driven by dynamic geometric deformation of the GO fiber shell due to solvent dynamics (Fig. 5f). The findings highlighted the potential for creating structurally robust materials with unchanged density and mechanical strength upon fusion, enabling higher load capacities. Furthermore, the application of GO coating to traditional fibers enhances their functionality with reversible fusion-fission properties, broadening the scope of their use. This research signifies a pivotal advancement in materials science, indicating potential for fields requiring dynamic, stimuli-responsive systems, and contributing to the development of recyclable materials. The diversity of emerging fabrication strategies reflects the ongoing innovation in GF synthesis, aiming to balance mechanical robustness, process simplicity, and multifunctionality for real-world deployment.

### 3 Light-weight electrical wires

Based on the low density and tunable structure/

component, GFs exhibit significant potential across a broad spectrum of applications, notably in the development of high-performance conductive wires with enhanced properties. For example, Xu et al. synthesized continuous graphene-metal hybrid fibers for light-weight wires through the wet-spinning process, utilizing giant GO combined with commercially available Ag nanowires. The resulting Ag nanowires-doped GFs exhibited a high electrical conductivity, reaching up to  $9.3 \times 10^4$  S/m, and a significant current capacity of  $7.1 \times 10^3$  A/cm<sup>2</sup> (Fig. 6a-c)<sup>[40]</sup>. Later, the same group introduced a comprehensive defect engineering strategy to prepare GF with exceptional stiffness measured at  $\sim 282$  GPa, alongside a mechanical tensile strength of 1.45 GPa. High electrical conductivity ( $\sim 0.8 \times 10^6$  S/m) and outstanding ampacity ( $\sim 2.3 \times 10^{10}$  A/m<sup>2</sup>) were also achieved (Fig. 6d-g)<sup>[13]</sup>. A straightforward two-zone vapor transport technique was developed for synthesizing chemically doped GFs (Fig. 6h), which had  $\sim 0.77 \times 10^7$  S/m for Fe-doped GF,  $1.50 \times 10^7$  S/m for Br doped GF, and  $2.24 \times 10^7$

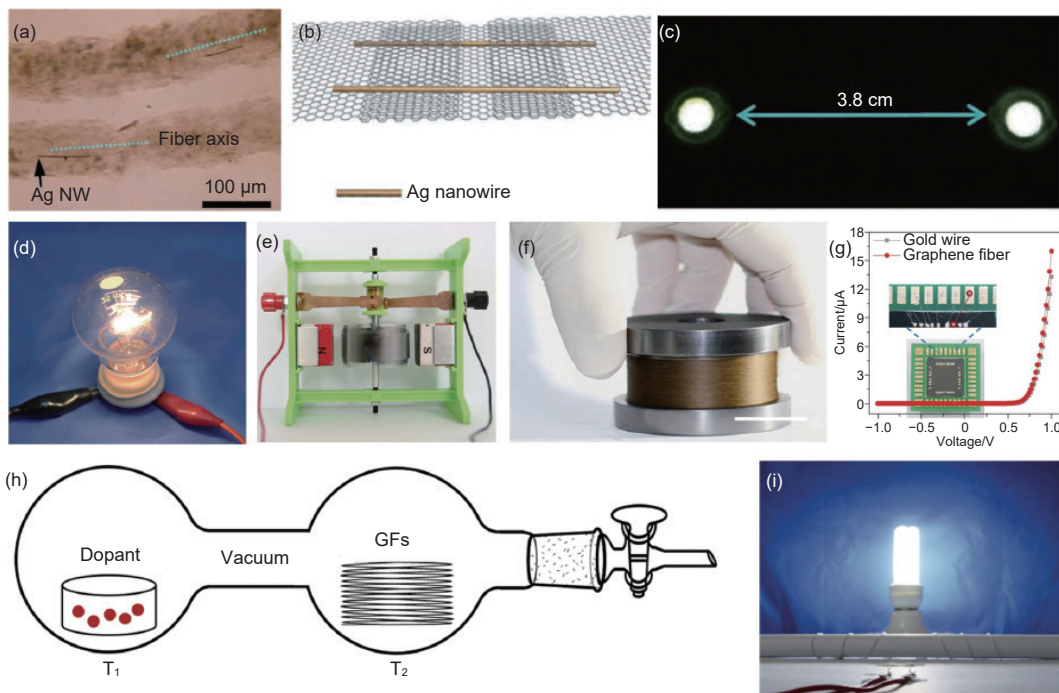


Fig. 6 GF wires and functional fabrics. (a-c) Optical depiction in ambient illumination of Ag nanowires-doped GFs. (b) Diagrammatic representations of the molecular doping process facilitated by Ag NWs. (c) Operational conditions of the stretchable circuit based on Ag nanowires-doped GFs. Reproduced with permission, Copyright 2013, Wiley<sup>[40]</sup>. (d-g) An operational incandescent bulb utilizing GF as a substitute for the tungsten filament. Reproduced with permission, Copyright 2016, Wiley<sup>[13]</sup>. (h, i) Schematic representation of the process for producing chemically doped GFs through a dual-zone vapor transport technique.

Reproduced with permission, Copyright 2016, Wiley<sup>[19]</sup>

S/m for K-doped GF. The remarkable increase in conductivity was attributed to the enhanced carrier concentration of post-doping, combined with the inherent high carrier mobility derived from graphene sheets<sup>[19]</sup>. Furthermore, a soft and transparent film was demonstrated by the integration of a network of GFs into a polydimethylsiloxane (PDMS) matrix. A magnetic GF wire was easily fabricated by adding Fe<sub>3</sub>O<sub>4</sub> nanoparticles in GO dispersion through ultrasonication, and then conducting hydrothermal treatment within pipelines for the in-situ integration of Fe<sub>3</sub>O<sub>4</sub> nanoparticles into the interlayer of graphene sheets<sup>[6]</sup>.

## 4 Fibrous energy harvesters

### 4.1 GF-based fibrous solar cells

Photovoltaic devices, traditionally composed of stiff panels, are ill-suited for scenarios demanding adaptability, such as portable and sophisticatedly integrated gadgets. Consequently, the exploration of flexible organic photovoltaics has emerged as a promising avenue of research aimed at catering to these specific needs. Utilizing a cost-efficient and practical solution process, Yang et al. transformed graphene into flexible fibers, which demonstrated a density of 0.61 g/cm<sup>3</sup>, a tensile strength ranging from 10<sup>2</sup> to 10<sup>3</sup> MPa, and an electrical conductivity between 10<sup>2</sup> and 10<sup>3</sup> S/cm. These GFs were further enhanced by the electrodeposition of platinum nanoparticles, enabling them to act as a counter electrode, while a titanium wire infused with vertically aligned titania nanotubes served as the working electrode (Fig. 7a). By intertwining these 2 electrodes, GF-based dye-sensitized photovoltaic device capable of efficiently harvesting light from all directions was successfully created (Fig. 7b). The exceptional flexibility, mechanical robustness, and electrical conductance of the graphene composite fibers culminated in achieving a certified maximum energy conversion efficiency of 8.45%, setting a new benchmark for the efficiency of wire-shaped photovoltaic devices<sup>[41]</sup>.

### 4.2 GF-based fibrous TE

The high electrical conductivity, tunable structure, and excellent flexibility of GF make it particu-

larly suitable for creating fiber-shaped TE generators. These generators, which convert temperature differences into electrical energy, are increasingly sought after for their potential in sustainable energy solutions. Initial studies in 2016 revealed GF's promise in TE applications, showcasing specific values for its Seebeck coefficient (ranging from -3.9 to 0.8  $\mu\text{V}\cdot\text{K}^{-1}$ ) and the thermoelectric figure of merit (ZT)<sup>[42]</sup>. However, the quest to further enhance these properties led to various innovative doping strategies. Introducing poly(3,4-ethylenedioxythiophene) : poly(styrenesulfonate) (PEDOT:PSS), bromine, and polyethyleneimine ethoxylated (PEIE) into GF has shown significant improvements in the TE performance<sup>[43-45]</sup>. Notably, the creation of PEDOT:PSS/graphene hybrid fibers through shape-confined hydrothermal methods demonstrated enhanced electrical conductivity and Seebeck coefficient ( $\sim 17.4 \mu\text{V}\cdot\text{K}^{-1}$ )<sup>[44]</sup>, by reducing the charge carrier transport barriers after the doping process (Fig. 7c).

The development of integrated p-n connected all-GFs marked a notable advance in this field (Fig. 7d)<sup>[43]</sup>. These fibers displayed improved ZT and power factor values and could be woven into flexible substrates like PDMS to create wearable TE generators. Such generators have shown impressive output power at room temperature, underscoring their potential in wearable technology. Bromine-doped GFs have set new benchmarks in TE performance, surpassing both undoped GFs and those composed solely of graphene or carbon nanotubes. The enhancements in these materials can be attributed to the dual effect of bromine doping, which not only lowers thermal conductivity through increased phonon scattering but also raises the Seebeck coefficient and electrical conductivity by adjusting the Fermi level. Despite these breakthroughs, GF-based TE generators still face challenges in transitioning from the laboratory to practical applications, a high temperature difference to achieve optimal TE performance, limitations in terms of scalability and mechanical compliance<sup>[44]</sup>. The future of GF in TE applications hinges on continued innovation in material science and engineering to en-

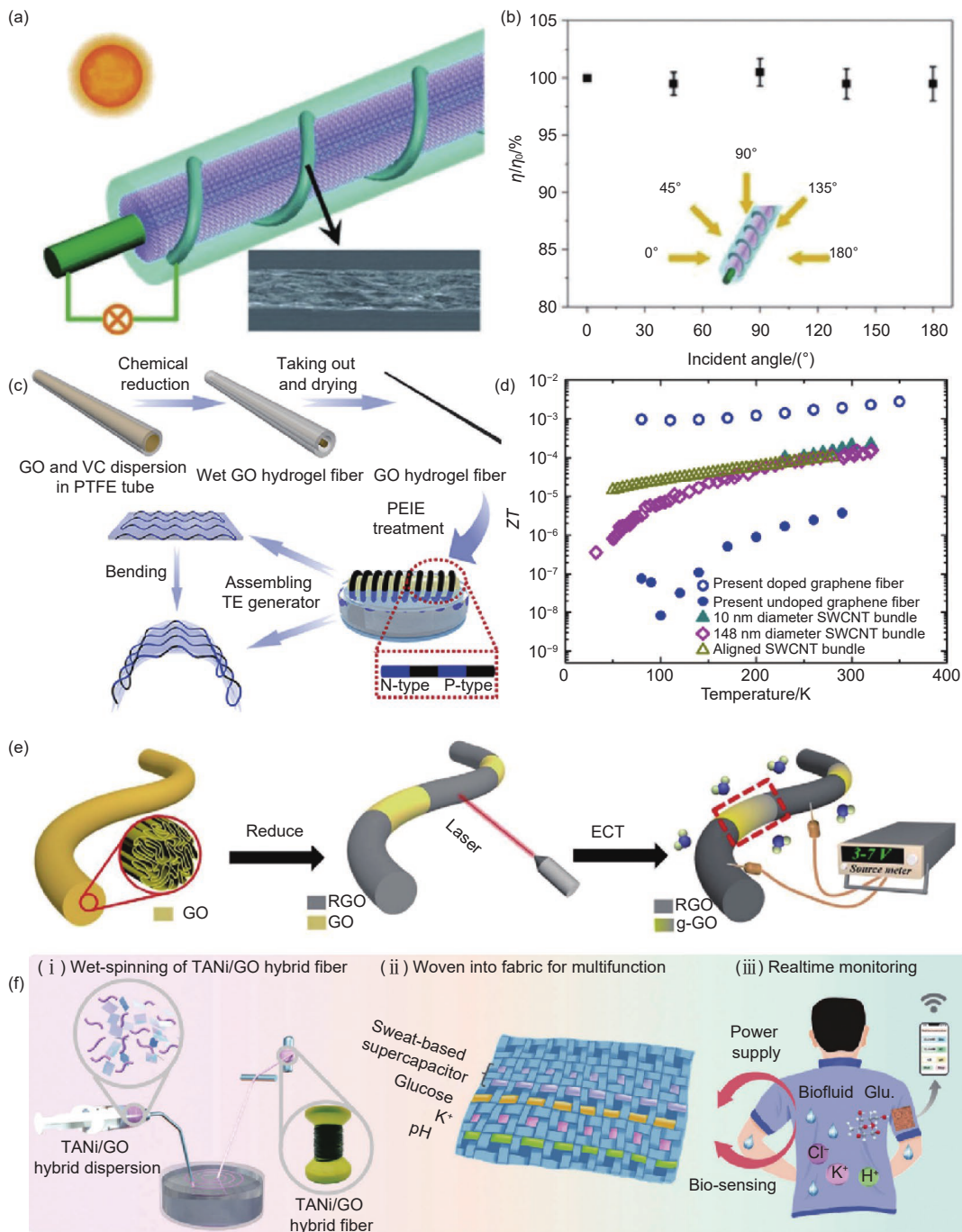


Fig. 7 (a, b) A dye-sensitized photovoltaic cell fabricated using a graphene/Pt composite fiber and a titanium wire. Reproduced with permission, Copyright 2013, Wiley<sup>[41]</sup>. (c) Graphical representation detailing the methodology for constructing a cohesive p-n junction GF. Reproduced with permission, Copyright 2019, Elsevier<sup>[44]</sup>. (d) The variation in the figure of merit for the evaluated GFs contingent upon temperature. Reproduced with permission, Copyright 2018, Springer publications<sup>[43]</sup>. (e) The construction process of a GF MEG. Reproduced with permission, Copyright 2017, Elsevier<sup>[20]</sup>. (f) Built-in potential GF MEG for bio-sensing. Reproduced with permission, Copyright 2023, Wiley<sup>[45]</sup>

hance its properties while addressing its current limitations. While current advances have validated the potential of GF-based TE devices, further breakthroughs in dopant selection and fiber integration are essential to meet the demands of practical energy harvesting systems.

### 4.3 GF-based fibrous MEG

Water, as a recyclable resource, is crucial for life and represents the planet's most abundant energy carrier, with 71% of Earth's surface being covered by water and absorbing 35% of solar energy. This immense energy potential, if efficiently harnessed, could

satisfy global energy demands<sup>[46]</sup>. In 2015, Qu's team first showcased a novel GO film-based MEG, effectively transforming moisture energy into electrical energy<sup>[47]</sup>. This groundbreaking work significantly heightened interest among researchers in the potential of moisture-enabled electricity generation<sup>[48–52]</sup>. Following this, a coaxial GF-based MEG was developed, featuring a core silver wire electrode encased in a GO layer for power generation, complemented by a secondary silver wire electrode<sup>[53]</sup>. This unique coaxial design promotes directional moisture diffusion and ionized  $H^+$  movement, resulting in a power density of  $0.21 \mu W cm^{-2}$ , an open-circuit voltage of approximately 0.3 V, and a short-circuit current density of about  $0.7 \mu A cm^{-2}$  under moisture conditions. The adaptability of this GF-based MEG to various forms and integration into flexible fabrics for wearable, self-powered electronics highlights its innovative application potential. In another work, an electrochemical treatment process was used to regulate the concentration of oxygen-containing groups in a GO fiber, creating a gradient oxygen-containing GO region. With graphene/gradient oxygen-containing GO/graphene structure, the GF-based MEG facilitated the formation of a concentration gradient of free  $H^+$  upon moisture exposure, leading to a stable potential as  $H^+$  migrated, generating current and voltage under specific humidity conditions. For example, the output voltage was 110–335 mV and the current density was  $0.19–1.06 mA cm^{-2}$  depending on the environment humidity. It also exhibited good mechanical flexibility, and the output voltage remained 95% of the initial value after 1000 bends<sup>[20]</sup>. Recently, similar built-in potential strategy was employed for the development of a high-performance uniaxial MEG with a core of poly(3,4-ethylenedioxythiophene) (PEDOT) and a gel shell composed of poly(diallyldimethylammonium chloride) and sodium alginate, which demonstrated performance of an output voltage of  $\sim 0.8 V$ , a maximum current density of  $1.05 mA/cm^2$ , and a power density of  $184 \mu W/cm^2$ <sup>[54]</sup>. These fibrous MEGs were successfully embedded into cloth to power an artificial synaptic device by mimicking the action potential

of a synapse under ambient conditions, showing tremendous potential in human–machine interactions and heralding new avenues in bioelectronic applications. These findings exemplify the synergy between material innovation and device design in exploiting ambient moisture for sustainable, wearable power solutions.

## 5 Summary and outlook

Recent studies have demonstrated the feasibility of assembling graphene nanosheets into continuous macroscopic fibers through various processing techniques, offering a potential pathway to harness graphene's exceptional mechanical and electrical properties at larger, more practical scales based on diverse GFs<sup>[55–60]</sup>. The fabrication of these GFs primarily involves overcoming 2 critical technical barriers: achieving controlled alignment of individual nanosheets to optimize load transfer and electrical pathways, and establishing strong interfacial bonding between adjacent nanosheets to ensure structural integrity. Current research in this field is actively exploring several promising approaches to refine these fabrication techniques, with particular emphasis on improving the mechanical robustness and electrical conductivity.

While these graphene-based fibers have demonstrated interesting characteristics that make them potentially useful for applications such as flexible conductors, thermal interface materials, or reinforcement elements in composites, their practical implementation still faces several significant hurdles. The most pressing challenges include developing scalable production methods that can maintain consistent quality over large volumes, ensuring performance reliability under various environmental conditions, and achieving cost-effectiveness compared to existing carbon fiber technologies. Additionally, researchers are working to better understand the fundamental structure-property relationships in these materials, particularly how processing parameters affect the final fiber characteristics at multiple length scales.

The field continues to evolve rapidly as new

characterization techniques and computational modeling approaches provide deeper insights into the assembly mechanisms and performance limitations of graphene-based fibers. Current research directions include exploring alternative precursor materials, developing more precise alignment control methods, and investigating novel post-processing treatments to enhance specific properties. As these fundamental studies progress and processing technologies mature, graphene-based fibers may find niche applications where their unique combination of properties offers distinct advantages over conventional materials, though widespread adoption will likely require further advancements in both performance and manufacturability.

## Acknowledgements

This work was supported by National Natural Science Foundation of China (52090032, 52350362, T2596012, 52022051) and National Key R&D Program of China (2024YFF0506000).

## References

- [ 1 ] Bolotin K I, Sikes K J, Jiang Z, et al. Ultrahigh electron mobility in suspended graphene[J]. *Solid State Communications*, 2008, 146(9-10): 351-355.
- [ 2 ] Balandin A A, Ghosh S, Bao W Z, et al. Superior thermal conductivity of single-layer graphene[J]. *Nano Letters*, 2008, 8(3): 902-907.
- [ 3 ] Geim A K. Graphene: status and prospects[J]. *Science*, 2009, 324(5934): 1530-1534.
- [ 4 ] Lee C, Wei X D, Kysar J W, et al. Measurement of the elastic properties and intrinsic strength of monolayer graphene[J]. *Science*, 2008, 321(5887): 385-388.
- [ 5 ] Xu Z, Gao C. Graphene chiral liquid crystals and macroscopic assembled fibres[J]. *Nature Communications*, 2011, 2: 571.
- [ 6 ] Dong Z L, Jiang C C, Cheng H H, et al. Facile fabrication of light, flexible and multifunctional graphene fibers[J]. *Advanced Materials*, 2012, 24(14): 1856-1861.
- [ 7 ] Li P, Liu Y J, Shi S Y, et al. Highly crystalline graphene fibers with superior strength and conductivities by plasticization spinning[J]. *Advanced Functional Materials*, 2020, 30(52): 2006584.
- [ 8 ] Xin G, Yao T K, Sun H T, et al. Highly thermally conductive and mechanically strong graphene fibers[J]. *Science*, 2015, 349(6252): 1083-1087.
- [ 9 ] Xu Z, Gao C. Graphene in macroscopic order: liquid crystals and wet-spun fibers[J]. *Accounts of Chemical Research*, 2014, 47(4): 1267-1276.
- [ 10 ] Chen L, He Y L, Chai S G, et al. Toward high-performance graphene fibers[J]. *Nanoscale*, 2013, 5(13): 5809-5815.
- [ 11 ] Sheng Z Z, Liu Z W, Hou Y L, et al. The rising aerogel fibers: status, challenges, and opportunities[J]. *Advanced Materials*, 2023, 10(9): 2205762.
- [ 12 ] Li M C, Zhang X H, Wang X, et al. Ultrastrong graphene-based fibers with increased elongation[J]. *Nano Letters*, 2016, 16(10): 6511-6515.
- [ 13 ] Xu Z, Liu Y J, Zhao X L, et al. Ultrastiff and strong graphene fibers via full-scale synergetic defect engineering[J]. *Advanced Materials*, 2016, 28(30): 6449-6456.
- [ 14 ] Li P, Wang Z Q, Qi Y X, et al. Bidirectionally promoting assembly order for ultrastiff and highly thermally conductive graphene fibres[J]. *Nature Communications*, 2024, 15(1): 409.
- [ 15 ] Zhao Y, Jiang C C, Hu C G, et al. Large-scale spinning assembly of neat, morphology-defined, graphene-based hollow fibers[J]. *ACS Nano*, 2013, 7(3): 2406-2412.
- [ 16 ] Hu C, Zhao Y, Cheng H H, et al. Graphene microtubings: controlled fabrication and site-specific functionalization[J]. *Nano Letters*, 2012, 12(11): 5879-5884.
- [ 17 ] Li X M, Zhao T S, Wang K L, et al. Directly drawing self-assembled, porous, and monolithic graphene fiber from chemical vapor deposition grown graphene film and its electrochemical properties[J]. *Langmuir*, 2011, 27(19): 12164-12171.
- [ 18 ] Lee K, Do M, Seo Y C, et al. Wet-to-dry hybrid spinning of graphene fiber inspired by spider silk production mechanisms[J]. *Advanced Materials Interfaces*, 2018, 5(21): 1800585.
- [ 19 ] Liu Y, Xu Z, Zhan J M, et al. Superb electrically conductive graphene fibers via doping strategy[J]. *Advanced Materials*, 2016, 28(36): 7941-7947.
- [ 20 ] Liang Y, Zhao F, Cheng Z H, et al. Self-powered wearable graphene fiber for information expression[J]. *Nano Energy*, 2017, 32: 329-335.
- [ 21 ] Qiu H, Qu X, Zhang Y, et al. Robust PANI@MXene/GQDs-based fiber fabric electrodes via microfluidic wet-fusing spinning chemistry[J]. *Advanced Materials*, 2023, 35(38): 2302326.
- [ 22 ] Xie L, Min M, Ye L, et al. Interfacial enhancement enables highly conductive reduced graphene oxide-based yarns for efficient electromagnetic interference shielding and thermal regulation[J]. *Carbon*, 2024, 230: 119655.
- [ 23 ] Jiang X, Ding T, Quan J, et al. High-performance graphene fiber supercapacitors with controlled pore architecture via in-situ drawing process[J]. *Carbon*, 2025, 238: 120254.
- [ 24 ] Huang W, Xu Y, Yang Y, et al. Wearable sensor for continuous monitoring multiple biofluids: improved performances by conductive metal-organic framework with dual-redox sites on flexible graphene fiber microelectrode[J]. *Advanced Functional Materials*, 2025, 2424018.

- [ 25 ] Xia Z and Shao Y L. Wet spinning assembled graphene fiber: Processing, structure, property, and smart applications[J]. *Acta Physico-chimica Sinica*, 2022, 38(9): 2103046.
- [ 26 ] Jian M, Zhang Y, and Liu Z. Graphene fibers: Preparation, properties, and applications[J]. *Acta Physico-chimica Sinica*, 2022, 38(2): 2007093.
- [ 27 ] Ding L, Xu T, Zhang J, et al. Covalently bridging graphene edges for improving mechanical and electrical properties of fibers[J]. *Nature Communications*, 2024, 15(1): 4880.
- [ 28 ] Yu D, Goh K, Wang H, et al. Scalable synthesis of hierarchically structured carbon nanotube-graphene fibres for capacitive energy storage[J]. *Nature Nanotechnology*, 2014, 9(7): 555-562.
- [ 29 ] Zhang Y, Zhang L Y, Zhou C W. Review of chemical vapor deposition of graphene and related applications[J]. *Accounts of Chemical Research*, 2013, 46(10): 2329-2339.
- [ 30 ] Chen T, Dai L M. Macroscopic graphene fibers directly assembled from CVD-grown fiber-shaped hollow graphene tubes[J]. *Angewandte Chemie-International Edition*, 2015, 54(49): 14947-14950.
- [ 31 ] Zeng J, Ji X X, Ma Y H, et al. 3D graphene fibers grown by thermal chemical vapor deposition[J]. *Advanced Materials*, 2018, 30(12): 1705380.
- [ 32 ] Li W, Liang F, Sun X, et al. Graphene-skinned alumina fiber fabricated through metalloidal-catalytic graphene CVD growth on nonmetallic substrate and its mass production[J]. *Nature Communications*, 2024, 15(1): 6825.
- [ 33 ] Feng L, Chang Y, Zhong J, et al. Dry spin graphene oxide fibers: mechanical/electrical properties and microstructure evolution[J]. *Scientific Reports*, 2018, 8(1): 10803.
- [ 34 ] Tian Q S, Xu Z, Liu Y J, et al. Dry spinning approach to continuous graphene fibers with high toughness[J]. *Nanoscale*, 2017, 9(34): 12335-12342.
- [ 35 ] Heim M, Keerl D, Scheibel T, Spider silk: from soluble protein to extraordinary fiber[J]. *Angewandte Chemie-International Edition*, 2009, 48(20): 3584-3596.
- [ 36 ] Hagn F, Eisoldt L, Hardy J G, et al. A conserved spider silk domain acts as a molecular switch that controls fibre assembly[J]. *Nature*, 2010, 465(7295): 239-242.
- [ 37 ] Jang E Y, Carretero-González J, Choi A, et al. Fibers of reduced graphene oxide nanoribbons[J]. *Nanotechnology*, 2012, 23(23): 235601.
- [ 38 ] Han Z, Wang J Q, Liu S P. Electrospinning of neat graphene nanofibers[J]. *Advanced Fiber Materials*, 2022, 4(2): 268-279.
- [ 39 ] Chang D, Liu J R, Fang B, et al. Reversible fusion and fission of graphene oxide-based fibers[J]. *Science*, 2021, 372(6542): 614-617.
- [ 40 ] Xu Z, Liu Z, Sun H Y, et al. Highly electrically conductive Ag-doped graphene fibers as stretchable conductors[J]. *Advanced Materials*, 2013, 25(23): 3249-3253.
- [ 41 ] Yang Z, Sun H, Chen T, et al. Photovoltaic wire derived from a graphene composite fiber achieving an 8.45% energy conversion efficiency[J]. *Angewandte Chemie-International Edition*, 2013, 52(29): 7545-7548.
- [ 42 ] Ma W, Liu Y, Yan S, et al. Systematic characterization of transport and thermoelectric properties of a macroscopic graphene fiber[J]. *Nano Research*, 2016, 9(11): 3536-3546.
- [ 43 ] Ma W, Liu Y J, Yan S, et al. Chemically doped macroscopic graphene fibers with significantly enhanced thermoelectric properties[J]. *Nano Research*, 2018, 11(2): 741-750.
- [ 44 ] Lin Y, Liu J, Wang X D, et al. An integral p-n connected all-graphene fiber boosting wearable thermoelectric energy harvesting[J]. *Composites Communications*, 2019, 16: 79-83.
- [ 45 ] Tong X, Yang D, Hua T, et al. , Multifunctional fiber for synchronous bio-sensing and power supply in sweat environment[J]. *Advanced Functional Materials*, 2023, 33(30): 2301174.
- [ 46 ] Li X M, Feng G, Chen Y D, et al. Hybrid hydrovoltaic electricity generation driven by water evaporation[J]. *Nano Research Energy*, 2024, 3: e9120110.
- [ 47 ] Zhao F, Cheng H H, Zhang Z P, et al. Direct power generation from a graphene oxide film under moisture[J]. *Advanced Materials*, 2015, 27(29): 4351-4357.
- [ 48 ] Bai J X, Huang Y X, Cheng H H, et al. Moist-electric generation[J]. *Nanoscale*, 2019, 11(48): 23083-23091.
- [ 49 ] Xu J X, Wang P F, Bai Z Y, et al. Sustainable moisture energy[J]. *Nature Reviews Materials*, 2024, 9(10): 722-737.
- [ 50 ] Wang L F, Wang H Y, Wu C X, et al. Moisture-enabled self-charging and voltage stabilizing supercapacitor[J]. *Nature Communications*, 2024, 15(1): 4929.
- [ 51 ] Li P Y, Hu Y J, He W Y, et al. Multistage coupling water-enabled electric generator with customizable energy output[J]. *Nature Communications*, 2023, 14(1): 5702.
- [ 52 ] Sun Z Y, Wen X, Wang L M, et al. Emerging design principles, materials, and applications for moisture-enabled electric generation[J]. *eScience*, 2022, 2(1): 32-46.
- [ 53 ] Shao C, Gao J, Xu T, et al. Wearable fiberform hygroelectric generator[J]. *Nano Energy*, 2018, 53: 698-705.
- [ 54 ] Zan G T, Jiang W, Kim H, et al. A core-shell fiber moisture-driven electric generator enabled by synergetic complex coacervation and built-in potential[J]. *Nature Communications*, 2024, 15(1): 10056.
- [ 55 ] Zhu Z Y, Men Y, Zhang W J, et al. Versatile carbon-based materials from biomass for advanced electrochemical energy storage systems[J]. *eScience*, 2024, 4(5): e100249.
- [ 56 ] Cheng H H, Hu C G, Zhao Y, et al. Graphene fiber: a new material platform for unique applications[J]. *NPG Asia Materials*, 2014, 6: e113.
- [ 57 ] Liu Y Z, Li Y F, Yang Y G, et al. Preparation and properties of graphene oxide-carbon fiber/phenolic resin composites[J]. *New*

- [Carbon Materials](#), 2012, 27(5): 377-384.
- [ 58 ] He W Y, Cheng H H, Qu L T. Progress on carbonene fibers for energy devices[J]. *Acta Physico-Chimica Sinica*, 2022, 38(9): 2203004.
- [ 59 ] Ci H N, Shi Z X, Wang M L, et al. A review in rational design of graphene toward advanced Li-S batteries[J]. *Nano Research Energy*, 2022, 2(2): e9120054.
- [ 60 ] Abay Z M, Wei Y X, Tang Z G, et al. Versatile MXene/(GO-AgNWs) electronic textile enabled by mixed-scale assembly strategy[J]. *Nano Energy*, 2025, 139: 110963.